Cellular Prion Protein Promotes *Brucella* Infection into Macrophages

Masahisa Watarai,[1] Suk Kim,[1] Janchivdorj Erdenebaatar,[1] Sou-ichi Makino,[1] Motohiro Horiuchi,[2] Toshikazu Shirahata,[1] Suehiro Sakaguchi,[3] and Shigeru Katamine[3]

[1]*Department of Applied Veterinary Science and* [2]*Research Center for Protozoan Diseases, Obihiro University of Agriculture and Veterinary Medicine, Hokkaido 080-8555, Japan*

[3]*Department of Molecular Microbiology and Immunology, Nagasaki University Graduate School of Biomedical Sciences, Nagasaki 852-8523, Japan*

The Journal of Experimental Medicine

Abstract

The products of the *Brucella abortus virB* gene locus, which are highly similar to conjugative DNA transfer system, enable the bacterium to replicate within macrophage vacuoles. The replicative phagosome is thought to be established by the interaction of a substrate of the VirB complex with macrophages, although the substrate and its host cellular target have not yet been identified. We report here that Hsp60, a member of the GroEL family of chaperonins, of *B. abortus* is capable of interacting directly or indirectly with cellular prion protein (PrP^C) on host cells. Aggregation of PrP^C tail-like formation was observed during bacterial swimming internalization into macrophages and PrP^C was selectively incorporated into macropinosomes containing *B. abortus*. Hsp60 reacted strongly with serum from human brucellosis patients and was exposed on the bacterial surface via a VirB complex–associated process. Under in vitro and in vivo conditions, Hsp60 of *B. abortus* bound to PrP^C. Hsp60 of *B. abortus*, expressed on the surface of *Lactococcus lactis*, promoted the aggregation of PrP^C but not PrP^C tail formation on macrophages. The PrP^C deficiency prevented swimming internalization and intracellular replication of *B. abortus*, with the result that phagosomes bearing the bacteria were targeted into the endocytic network. These results indicate that signal transduction induced by the interaction between bacterial Hsp60 and PrP^C on macrophages contributes to the establishment of *B. abortus* infection.

Key words: Hsp60 • type IV secretion • macropinocytosis • intracellular replication • brucellosis

Introduction

Brucella species are Gram-negative bacteria that cause brucellosis with pathological manifestations of arthritis, endocarditis, and meningitis as well as undulant fever in humans and abortion and infertility in numerous domestic and wild mammals (1). The bacterium is endemic in many developing countries and is responsible for large economic losses and chronic infections in humans (2). *Brucella* species are facultative intracellular pathogens that survive within a variety of cells, including macrophages. The virulence of these species and the establishment of chronic infection are thought to be due essentially to their ability to avoid the killing mechanisms within macrophages (3). However, the molecular mechanisms accounting for these properties are not understood completely.

Recent studies with nonprofessional phagocyte HeLa cells have confirmed these observations, showing that *Brucella* inhibits phagosome–lysosome fusion and transits through an intracellular compartment that resembles autophagosomes. Bacteria replicate in a different compartment, containing protein markers normally associated with the endoplasmic reticulum, as shown by confocal microscopy and immunogold electron microscopy (4, 5).

Brucella internalizes into macrophages by swimming on the cell surface with generalized membrane ruffling for several minutes, a process termed "swimming internalization," after which the bacteria are enclosed by macropinosomes (6). In this period, the phagosomal membrane continues to

Address correspondence to Masahisa Watarai, Department of Applied Veterinary Science, Obihiro University of Agriculture and Veterinary Medicine, Inada-cho, Obihiro-shi, Hokkaido 080-8555, Japan. Phone: 81-155-49-5387; Fax: 81-155-49-5386; E-mail: watarai@obihiro.ac.jp

 J. Exp. Med. © The Rockefeller University Press • 0022-1007/2003/07/5/13 $8.00
Volume 198, Number 1, July 7, 2003 5–17
http://www.jem.org/cgi/doi/10.1084/jem.20021980

maintain a dynamic state. Lipid raft–associated molecules, such as glycosylphosphatidylinositol (GPI)*-anchored proteins, GM1 gangliosides, and cholesterol, have been shown to be selectively incorporated into macropinosomes containing *Brucella abortus*. In contrast, late endosomal marker lysomal-associated membrane protein (LAMP)-1 and host cell transmembrane proteins are excluded from the macropinosomes. The disruption of lipid rafts on macrophages markedly inhibits the VirB-dependent macropinocytosis and intracellular replication (6). These results indicated that the entry route of *B. abortus* into the macrophages determined the intracellular fate of the bacteria that was modulated by lipid rafts (6, 7).

The operon coding for export mechanisms specializing in transferring a variety of multimolecular complexes across the bacterial membrane to the extracellular space or into other cells has been described (8). These complexes, named type IV secretion systems, are also found in *B. abortus* (*virB* genes; 9–11). This operon comprises 13 open reading frames that share homology with other bacterial type IV secretion systems involved in the intracellular trafficking of pathogens. Type IV secretion systems export three types of substrates: (a) DNA conjugation intermediates, (b) the multisubunit pertussis toxin, and (c) monomeric proteins including primase, RecA, the *Agrobacterium tumefaciens* VirE2 and VirF proteins, and the *Helicobactor pylori* CagA protein (8). However, the substrates of the VirB secretion system of *B. abortus* and the target of the effector in host cells remain undefined.

In this study, we investigated the effector protein secreted by the type IV secretion systems and its receptor on the host plasma membrane. Our results implied that heat shock protein Hsp60 of *B. abortus* had an effector-like function, which was expressed on the bacterial surface by the type IV secretion–associated manner. The cellular prion protein (PrP^C) was identified as a receptor for the Hsp60. This receptor–ligand interaction regulates the establishment of *B. abortus* infection.

Materials and Methods

Reagents. Gentamicin, protein A–Sepharose 4B beads, and 4′,6-diamidino-2-phenylindole (DAPI) were obtained from Sigma-Aldrich. Ni-NTA agarose beads were obtained from QIAGEN. Alexa Fluor 594-streptavidin, Cascade blue goat anti–rabbit IgG, and Texas Red goat anti–rat IgG were obtained from Molecular Probes, Inc. Rhodamine goat anti–rabbit or mouse IgG was obtained from ICN Pharmaceuticals. Anti–*B. abortus* polyclonal rabbit serum, aerolysin, and anti- PrP^C biotin-labeled mouse monoclonal antibody have been described (6, 12). Anti–mouse CD48 rat monoclonal antibody MRC OX-78 was obtained from Serotech. Anti–*Escherichia coli* GroEL mouse monoclonal antibody 9A1/2 was obtained from Calbiochem. Anti-Hsp60 rabbit polyclonal antibody was obtained from MBL International Corporation. Anti–glucose-6-phosphate dehydrogenase (G6PDH) goat polyclonal antibody was obtained from Cortex Biochem. *Brucella*-infected human, cattle, and sheep sera have been described (13). Anti–LAMP-1 rat monoclonal antibody 1D4B was obtained from the Developmental Studies Hybridoma Bank of the Department of Pharmacology and Molecular Sciences, Johns Hopkins University School of Medicine and the Department of Biology, University of Iowa.

Bacterial Strains and Media. All *B. abortus* derivatives were from 544 (ATCC23448), smooth virulent *B. abortus* biovar 1 strains. Ba598 (544 Δ*virB4*), Ba600 (544 GFP^+), and Ba604 (Δ*virB4* GFP^+) have been described (6, 14). *B. abortus* strains were maintained as frozen glycerol stocks and cultured on Brucella broth (Becton Dickinson) or Brucella broth containing 1.5% agar. Kanamycin was used at 40 μg/ml.

Construction of An In-Frame Deletion Mutant of virB2. pMAW24 (Δ*virB2*) was constructed by cloning two PCR fragments into SalI/SacI-cleaved pSR47s (14). Fragment 1 was a 1,609-bp SalI-BglII fragment spanning a site located 1,609 nucleotides upstream of the 5′ end of *virB2* to 6 nucleotides downstream from the 5′ end and was amplified by PCR using primers 5′-GTCGACATGACAGGCATATTTCAACGC-3′ (SalI site underlined) and 5′-AGATCTTTTCATGATCTTTATTCCTAA-3′ (BglII site underlined; nucleotide positions 1 and 1,614 are available from GenBank/EMBL/DDBJ under accession no. AF226278, respectively; reference 10). Fragment 2 was a 1,600-bp BamHI-SacI fragment spanning the region starting 6 nucleotides upstream of the 3′ end of *virB2* to a position 1,594 nucleotides downstream from the 3′ end and was amplified using primers 5′-GGATCCAGGTAAAGGGACACAGATCAT-3′ (BamHI site underlined) and 5′-GAGCTCCATCCCGCTTGCCTGCGCGGA-3′ (SacI site underlined; nucleotide positions 1,921 and 3,526 are available from GenBank/EMBL/DDBJ under accession no. AF226278, respectively; reference 10). pMAW24 (Δ*virB2*) was introduced into *E. coli* DH5α (λ*pir*) and then the plasmid was transferred into *B. abortus* 544 by electroporation (Gene Pulser; Bio-Rad Laboratories). Isolation of in-frame deletion mutant by the positive selection for sucrose resistance has been described (14).

pMAW25 (*virB2*$^+$) was constructed by cloning a PCR fragment into SalI/BamHI-cleaved pBBR1MCS-2 (15). The 707-bp EcoRI-BamHI PCR fragment spanned a site located 369 nucleotides upstream of the 5′ end of *virB2* to a position 21 nucleotides downstream from the 3′ end (10) and was amplified using the primers 5′-GTCGACGTTATAGCGGCGGGCGGCGAC-3′ (SalI site underlined) and 5′-GGATCCGTTGTCATGATCTGTGTCCCT-3′ (BamHI site underlined).

Cell Culture. Bone marrow–derived macrophages from female BALB/c, C57BL/6, Ngsk, or Zrch PrP^C-deficient mice (16, 17), and PrP^C transgenic Ngsk PrP^C-deficient mice (18) were prepared as previously described (6, 14). After culturing in L cell–conditioned medium, the macrophages were replated for use by lifting cells in PBS on ice for 5 to 10 min, harvesting cells by centrifugation, and resuspending cells in RPMI 1640 containing 10% fetal bovine serum. The macrophages were seeded ($2–3 \times 10^5$ per well) in 24-well tissue culture plates for all assays.

Immunofluorescence Microscopy. Detection of intracellular bacteria, macropinosome formation, and fluorescence-labeled molecules by fluorescence microscopy have been described (6). In brief, *B. abortus* strains were grown to A600 = 3.2 in Brucella broth and used to infect mouse bone marrow–derived macrophages for various lengths of time at a multiplicity of infection of

*Abbreviations used in this paper: DAPI, 4′,6-diamidino-2-phenylindole; G6PDH, glucose-6-phosphate dehydrogenase; GPI, glycosylphosphatidylinositol; LAMP, lysomal-associated membrane protein; NPC1, Niemann-Pick type C1 gene; PrP, prion protein; PrP^C, cellular PrP; WASP, Wiskott-Aldrich syndrome protein.

20. Infected cells were fixed in periodate-lysine-paraformaldehyde containing 5% sucrose for 1 h at 37°C. Samples were washed three times in PBS and wells were successively incubated three times for 5 min in blocking buffer (2% goat serum in PBS) at room temperature.

All antibody-probing steps were for 1 h at 37°C. Samples were washed three times in PBS for 5 min and then permeabilized in −20°C methanol for 10 s. After incubating three times for 5 min with blocking buffer, samples were stained with each primary antibody. After washing three times for 5 min in blocking buffer, samples were stained simultaneously with each secondary antibody. Samples were placed in mounting medium and visualized by fluorescence microscopy.

100 macrophages were examined per coverslip to determine the total number of intracellular bacteria, macropinosome formation, and total number of bacteria within macropinosomes (6).

Determination of Efficiency of Bacterial Uptake and Intracellular Growth by Cultured Macrophages. To determine uptake of bacteria, mouse bone marrow–derived macrophages were infected with *B. abortus*. After 0, 5, 15, 25, and 35 min incubation at 37°C, macrophages were washed once with medium and incubated with 30 μg/ml gentamicin for 30 min. Macrophages were then washed three times with fresh medium and lysed with distilled water. CFUs were determined by serial dilutions on Brucella plates. Percentage protection was determined by dividing the number of bacteria surviving the assay by the number of bacteria in the infectious inoculum, as determined by viable counts.

To determine intracellular growth of bacteria, the infected macrophages were then washed once with medium and incubated with 30 μg/ml gentamicin. At different time points, cells were washed and lysed with distilled water and the number of bacteria was counted on plates of a suitable dilution (6).

Ni-NTA Agarose Pull-Down and Immunoprecipitation Assay. A fusion protein of Hsp60 tagged with six histidine residues at the NH_2 terminus was constructed using the QIAexpress system with pQE30 plasmid (QIAGEN). The fusion Hsp60 protein was purified by Ni-NTA chromatography.

For the pull-down assay, Ni-NTA agarose beads–bound Hsp60 (20 μg/ml) were added to 1 ml macrophage lysate ($\sim 10^9$ cells) prepared with lysis buffer (10 mM Tris-HCl, pH 7.6, 5 mM EDTA, 50 mM NaCl, 30 mM sodium pyrophosphate, 50 mM NaF, 1% Triton X-100, 0.1% SDS, 4 μg/ml leupeptin, 1 mM PMSF; reference 19), and the mixture was incubated at 37°C for 20 min. Ni-NTA agarose beads–bound PrP^C (20 μg/ml; reference 20) were added to 1 ml purified Hsp60 solution (20 μg/ml), and the mixture was incubated at 37°C for 20 min.

For immunoprecipitation assay, 20 μg/ml Hsp60 added to 1 ml macrophage lysate was incubated at 37°C for 20 min. The sample was then immunoprecipitated with the anti-PrP^C antibody and incubated at 4°C overnight. Protein A–Sepharose beads were added to the sample and incubated at room temperature for 1 h. Each protein or antibody (20 μg/ml) was added in reaction solution and incubated for 20 min before pull-down or immunoprecipitation for binding inhibition.

The precipitates were washed with PBS and analyzed by immunoblotting with either anti-Hsp60 or anti-PrP^C, and silver staining was performed using 2D-Silver Stain II (Daiichi Pure Chemicals).

Expression of Hsp60 on Lactococcus Lactis. pMAW30 (*B. abortus* $Hsp60^+$) or pMAW31 (*E. coli* $Hsp60^+$) was constructed by cloning a PCR fragment into KpnI/SacI- or SacI-cleaved pSECE1, which is a vector for the secretion of foreign protein to the cell surface of *L. lactis* (21). The 1,640-bp KpnI-SacI or 1,647-bp SacI PCR fragment spanned the *hsp60* gene of *B. abortus* (22) or *E. coli* (23) and was amplified using the primers 5′-GGTACCATGGCTGCAAAAGACGTAAAA-3′ (KpnI site underlined) and 5′-GAGCTCTTAGAAGTCCATGCCGCCCAT-3′ (SacI site underlined), or 5′-GAGCTCATGGCAGCTAAAGACGTAAAA-3′ (SacI site underlined) and 5′-GAGCTCTTACATCATGCCGCCCATGCC-3′ (SacI site underlined). Transformation of *L. lactis* IL1403 was performed according to the method of Holo and Nes (24).

Hsp60 Localization on Bacteria. Bacteria were grown to A600 = 3.2 in broth, collected by centrifugation, and fixed in 4% paraformaldehyde. Expression of Hsp60 on the *B. abortus* or *L. lactis* surface was confirmed by immunofluorescence microscopy with anti-Hsp60 monoclonal antibody (25). Immunofluorescence staining of permeabilized bacteria was performed as previously described (25).

ELISA. The ability of PrP^C to bind to Hsp60 on *L. lactis* was measured as follows. A 50-μl aliquot of $\sim 10^8$ *L. lactis* was placed into 96-well immuno plates (Nunc) and incubated at room temperature for 2 h. The sample was then removed and the wells were washed twice with PBS-0.05% Tween 20. 50 μl macrophage lysate (200 μg/ml) were added and the plate was incubated at 37°C for 1 h. The amount of bound PrP^C was determined by ELISA with anti-PrP^C antibody.

Time Lapse Video Microscopy. Bone marrow–derived macrophages were plated in Lab-Tek Chambered coverglass (Nunc) and incubated overnight in RPMI 1640 containing 10% FBS at 37°C in 5% CO_2. 2×10^6/ml bacteria were added to the chamber and then the chamber was placed on a heated microscope stage set to 37°C for observation using an Olympus IX70 inverted phase microscope with 100× UPlanApo lens fitted with phase contrast optics. The bacteria were allowed to settle passively onto the macrophages and images were captured over a 30-min period. The images were captured every 15 s using a cooled CCD camera (CoolSNAP; Roper Scientific) and processed using Openlab software (Improvision) on a Power Macintosh G4 computer.

Virulence In Mice. Virulence was determined by quantitating the survival of the strains in the spleen after 10 d. Groups of five mice were injected intraperitoneally with $\sim 10^4$ CFUs of brucellae in 0.1 ml saline. At 10 d after infection, their spleens were removed and homogenized in saline. Tissue homogenates were serially diluted with PBS and plated on Brucella agar to count the number of CFUs in each spleen.

Results

Tail Formation of PrP^C with Swimming Internalization of B. abortus. Our previous results showed that GPI-anchored proteins were selectively incorporated into macropinosomes containing *B. abortus* (Fig. 1; reference 6). To investigate further the membrane sorting process, the distribution of GPI-anchored proteins during swimming internalization of *B. abortus* was analyzed. Aerolysin from *Aeromonas hydrophila*, which binds to the GPI moiety of GPI-anchored proteins on the cell surface (26), was used as probe for the detection of GPI-anchored proteins. At 5 min after infection, aggregation of aerolysin-labeled GPI-anchored proteins showing tail-like formation was colocalized with swimming bacteria on the macrophage surface (Fig. 1). In contrast, no aggregation of CD48, which is a GPI-anchored protein, was observed at the same time

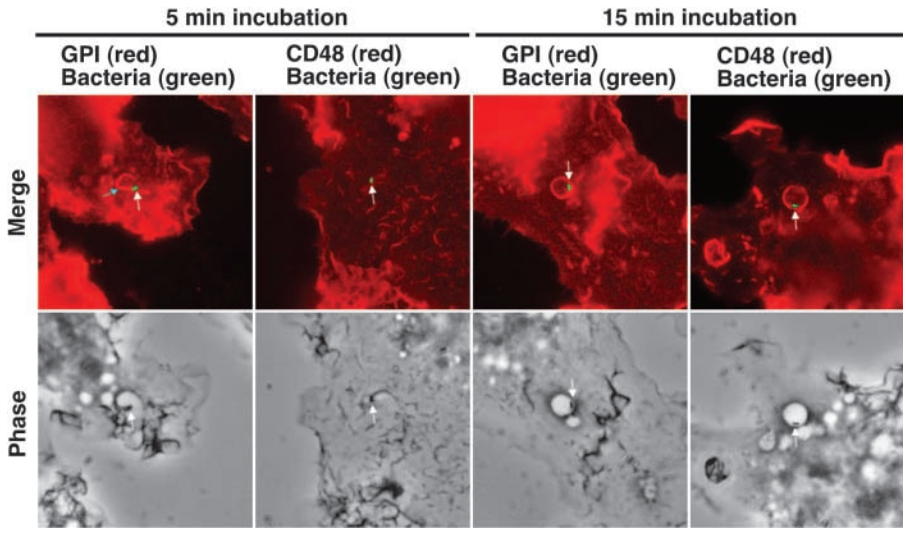

Figure 1. Tail formation of GPI-anchored proteins on the site of swimming internalization. Bone marrow–derived macrophages were incubated with *B. abortus* for 5 or 15 min, and GPI-anchored proteins were localized by immunofluorescence as described in Materials and Methods. Merged images of the GFP (green) and TRITC (red) channels up and down with phase contrast images of the same field are shown. Cells were probed with aerolysin for GPI-anchored proteins and with anti-CD48. White arrows point to bacteria and blue arrow points to tail-like aggregation of GPI-anchored proteins.

point (Fig. 1). Similar results were obtained for other GPI-anchored proteins, such as CD55 (unpublished data). However, when one GPI-anchored protein, PrP^C, was tested, colocalization of aggregated PrP^C tail and swimming bacteria was observed (Fig. 2 A). Sometimes, several PrP^C tails were observed from a single bacterium (Fig. 2 A). PrP^C was also incorporated into macropinosomes containing wild-type strain, but not *virB4* mutant, after 15 min incubation (Fig. 2 A).

To obtain the ratio of PrP^C tail formation, colocalization of PrP^C tail and internalized bacteria was quantitated microscopically at various times of incubation. *virB4* mutant was rapidly internalized, with most bacteria internalized before further incubation, but the internalization of wild-type strain was delayed (Fig. 2 B). Wild-type strain, but not *virB4* mutant, was present in macropinosomes transiently (Fig. 2 C). The kinetics and degree of association of the PrP^C tail with internalized wild-type strain showed maximal association after 5 min incubation (Fig. 2 D). The maximal association of PrP^C with phagosomes containing wild-type strain was observed after 15 min incubation (Fig. 2 E). In contrast, colocalization of PrP^C with *virB4* mutant was much less pronounced (Fig. 2, D and E). These results suggested that bacterial products secreted by the type IV system might aggregate PrP^C specifically and form tail structures during swimming internalization of *B. abortus*.

Surface Exposure of Hsp60 on B. abortus. To investigate bacterial factors associated with PrP^C tail formation, immunodominant proteins were examined by immunoblotting with human brucellosis sera, which recognized a major protein (60 kD) and two minor proteins (30~25 kD; Fig. 3 A). In a previous report (22), immunodominant Hsp60 reacted with sera from mice experimentally infected with *B. abortus*. Therefore, the 60-kD protein was expected to be Hsp60. To confirm this, purified Hsp60 of *B. abortus* was analyzed by immunoblotting with sera from human and animal brucellosis. As expected, Hsp60 reacted with serum from human, cattle, and sheep with naturally acquired brucellosis (Fig. 3 B). Mutant strains (Δ*virB2* and Δ*virB4*) also had immunoreactive Hsp60 (Fig. 3 A). To examine if Hsp60 was secreted into the external medium, culture supernatant of *B. abortus* was analyzed by immunoblotting. Immunoreactive proteins were not detected in culture supernatant (unpublished data). However, surface-exposed Hsp60 on wild-type strain, but not *virB2* and *virB4* mutants, was detected by immunofluorescence staining with anti-Hsp60 antibody (Fig. 3 C). Because introduction of complementing plasmid into each mutant restored surface expression of Hsp60, the expression of Hsp60 on the bacterial surface associates with the type IV secretion system (Fig. 3 C).

To demonstrate that, as above, the presence of Hsp60 on the bacterial surface did not result from wholesale relocalization of cytoplasmic leakage, a control experiment was performed. Surface exposure of G6PDH was determined by immunofluorescence microscopy. Antibody against G6PDH failed to react with bacterial cell surfaces. As it was not certain that the control antibody was able to react with bacterial cells in the immunofluorescence experiment, the antibody was used to probe bacteria in the presence or absence of permeabilization by hypotonic lysozyme treatment (25). Antibody against G6PDH reacted with permeabilized bacteria, but failed to react with bacterial cell surface (Fig. 3 D). Therefore, the surface exposure of Hsp60 is not caused by cytoplasmic leakage.

Interaction of PrP^C with Hsp60 of B. abortus. Because Hsp60 expressed on the bacterial surface by the type IV secretion system was most likely interacting with the target cell, we tested Hsp60 for its ability to bind to PrP^C on macrophages by pull-down assay with Hsp60 or PrP^C beads. Analysis of the precipitated proteins by immunoblotting with anti-PrP^C or Hsp60 antibody showed that a 29-kD PrP^C was associated with Hsp60, but not beads alone (Fig. 4, A and B). To confirm this association, Hsp60 was added to macrophage lysate and the proteins in the mixture were then immunoprecipitated with anti-PrP^C antibody. The

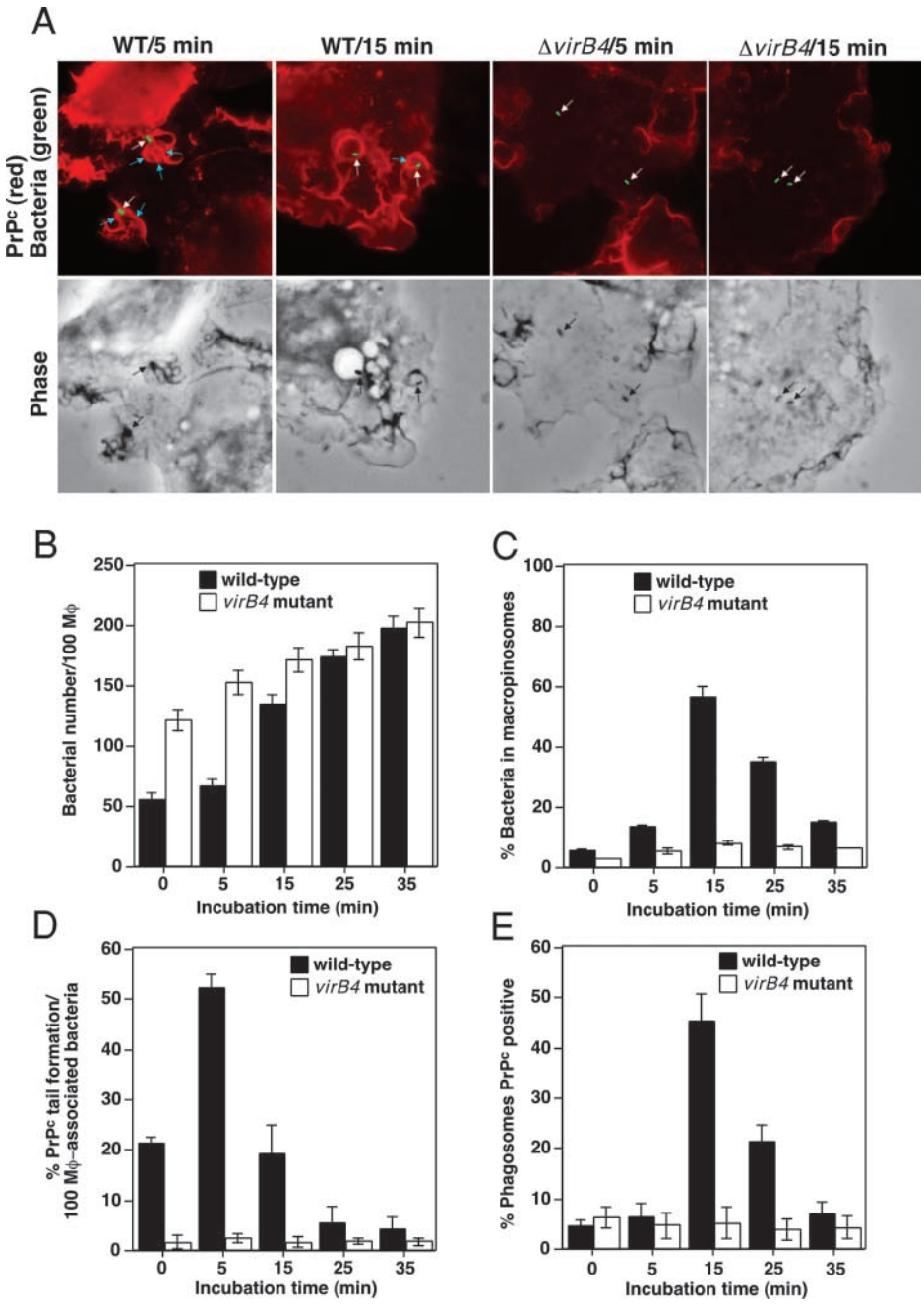

Figure 2. PrP^C tail formation at the site of swimming internalization. (A) Macrophages were incubated with *B. abortus* for 5 or 15 min, and PrP^C were localized by immunofluorescence as described in Materials and Methods. Merged images of the GFP (green) and TRITC (red) channels up and down with phase contrast images of the same field are shown. White arrows point to bacteria and blue arrows point to tail-like aggregation of PrP^C. (B–E) Wild-type (solid bars) or *virB4* mutant (open bars) were deposited onto macrophages and then incubated for the periods of time indicated. Uptake (B), macropinosome formation (C), PrP^C tail formation (D), or PrP^C positive phagosomes (E) was quantified as described in Materials and Methods. % PrP^C tail formation or % phagosomes PrP^C positive refers to the percentage of bacteria that showed costaining with the PrP^C tail or PrP^C-included phagosomes. 100 macrophages (B and C) or 100 bacteria (D and E) were examined per coverslip. Data are the average of triplicate samples from three identical experiments, and the error bars represent the standard deviation.

precipitated proteins were analyzed by immunoblotting with anti-Hsp60 antibody. The precipitates contained Hsp60 (Fig. 4 B). Because the anti-Hsp60 antibody did not recognize macrophages Hsp60, the antibody showed specific for bacterial Hsp60 (Fig. 4 B). This Hsp60 and PrP^C association was inhibited by the addition of anti-Hsp60 polyclonal antibody, purified Hsp60, or PrP^C (Fig. 4, A and B). These results indicated that the interaction between Hsp60 and PrP^C would be specific. The precipitated proteins were also analyzed by silver staining. The precipitates contained two major bands (60 and 29 kD) and two weak minor bands (74 and 27 kD; Fig. 4 C). These results suggested that Hsp60 bound to PrP^C mostly, but there is possibility that Hsp60 might interact indirectly with PrP^C mediated by other cellular components.

To further characterize Hsp60, distribution of Hsp60 in *B. abortus*–infected macrophages was analyzed by immunofluorescence microscopy. At 5 or 15 min after infection, Hsp60 colocalized with only the bacterial surface and was not detected in macrophage membrane or cytoplasm (Fig. 4 D).

To investigate if Hsp60 exposed on bacterial surface could aggregate PrP^C on macrophages, macrophages were infected with *L. lactis* expressing Hsp60 of *B. abortus* on its surface (Fig. 5 B), and then PrP^C was detected by immunofluorescence microscopy. After 5 min incubation, PrP^C

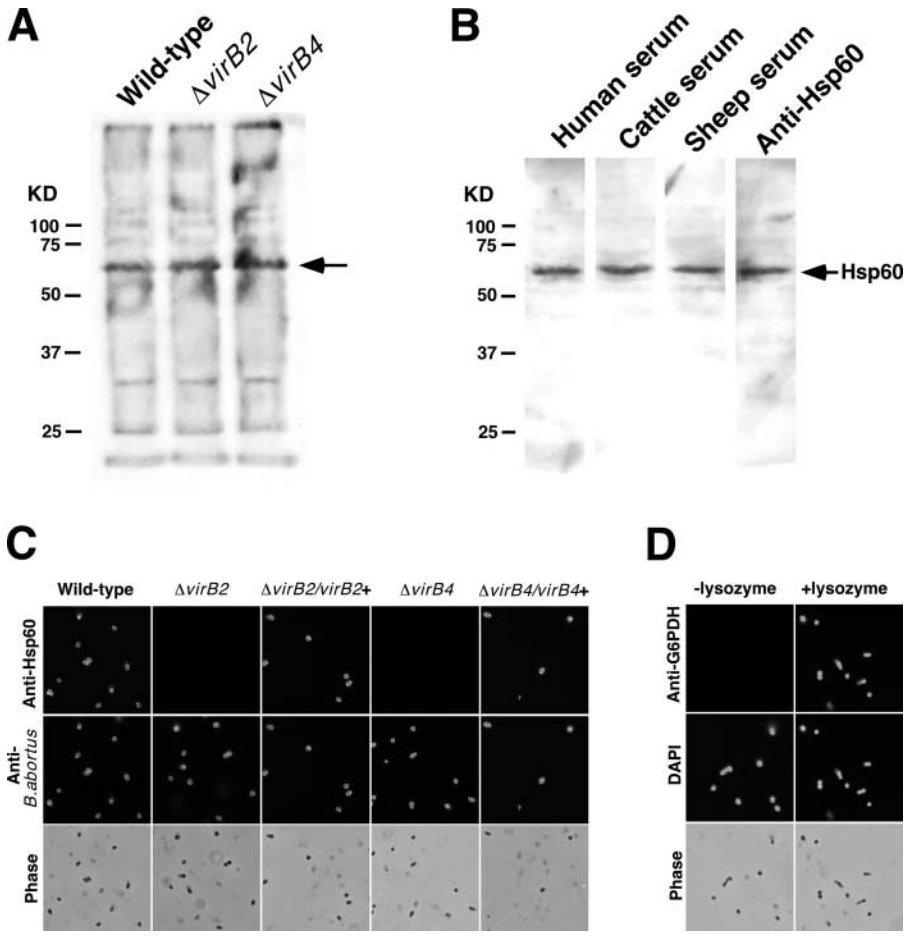

Figure 3. VirB complex–dependent surface expression of immunodominant Hsp60. Immunoblot analysis of whole cell lysates with serum from human brucellosis (A) and of purified Hsp60 with indicated serum (B). (C) Labeling of bacteria grown in vitro with antibody specific for Hsp60. Fluorescence microscopy of stained wild-type, *virB2*, or *virB4* mutant, and complemented strain for each mutant, with anti-Hsp60 (top) or anti–*B. abortus* (middle) and phase contrast microscopy of the corresponding microscopic fields (bottom) are shown. (D) Localization of G6PDH on permeabilized *B. abortus* by immunofluorescence microscopy. Bacteria were probed with anti-G6PDH (top) and stained for DNA with DAPI (middle) in either the absence (−lysozyme) or the presence (+lysozyme) of lysozyme, and phase contrast microscopy of the corresponding microscopic fields (bottom) are shown.

accumulated around internalized Hsp60$^+$ *L. lactis* but not Hsp60$^-$ *L. lactis* (Fig. 5 A). Quantitative data showed that >70% of *L. lactis* expressing Hsp60 colocalized with PrP^C at all time points (Fig. 5 D). PrP^C tail formation was not observed with either Hsp60$^+$ or Hsp60$^-$ *L. lactis*. *L. lactis* was seeded on the wells of a microtiter plate, macrophage lysate was added, and then binding activity was measured by ELISA with anti-PrP^C antibody. The binding of PrP^C to Hsp60 on the *L. lactis* surface was detected but not with Hsp60$^-$ *L. lactis* (Fig. 5 C). *L. lactis* expressing Hsp60 of *E. coli* also colocalized with PrP^C at all time points, but the percentage of colocalization was lower than Hsp60 of *B. abortus* (Fig. 5, C–E). These results suggested that Hsp60 expressed on the bacterial surface promoted accumulation of PrP^C, but is not sufficient for PrP^C tail formation.

Effect of PrP^C Deficiency on B. abortus Infection. To investigate the role of PrP^C on *B. abortus* infection, several phenotypes of *B. abortus* virulence were tested by using macrophages from Ngsk PrP^C-deficient mice (16). Time lapse videomicroscopy was used to follow the internalization of *B. abortus* by macrophages from parent or Ngsk PrP^C-deficient C57BL/6 mice. After contact of macrophages with *B. abortus*, bacteria showed swimming internalization in macrophages from parent mice (Fig. 6 A). The swimming of the bacteria on the macrophage surface lasted for several minutes with generalized plasma membrane ruffling before eventual enclosure in macropinosomes (Fig. 6 A). Contact of *B. abortus* with macrophages from Ngsk PrP^C-deficient mice, in contrast, resulted in much smaller ruffling that was restricted to the area near the bacteria. The ruffles associated with internalization of bacteria resulted in a more rapid uptake than observed for macrophages from parent mice (Fig. 6 B). 5 min after deposition on the macrophages from parent mice, *B. abortus* showed generalized actin polymerization around the site of bacterial binding, which could be observed by either phalloidin staining or phase contrast microscopy (Fig. 6 C). Macrophages from Ngsk PrP^C-deficient mice showed primarily small regions of phalloidin staining at sites of bacterial binding (Fig. 6 C).

The differences in rate of phagocytosis and macropinosome formation for parent or Ngsk PrP^C-deficient mice were quantitated microscopically at various times of incubation. The kinetics of bacterial internalization and macropinosome formation in macrophages from parent C57BL/6 mice were almost identical to those observed for macrophages from BALB/c mice (Figs. 2, B and C, and 7, A–C). Internalization of wild-type *B. abortus* into macrophages from Ngsk PrP^C-deficient mice, in contrast, was much quicker and macropinosome formation was hardly detectable (Fig. 7, D–F). The internalized wild-type strain did

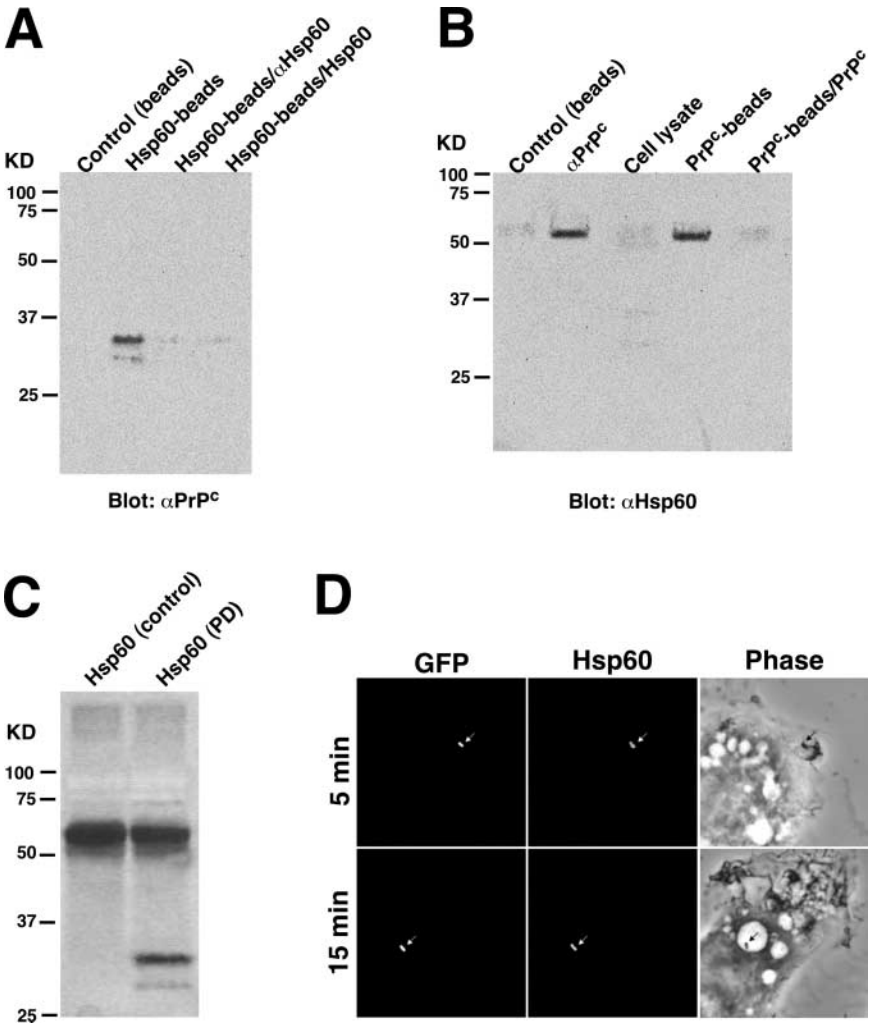

Figure 4. Binding of Hsp60 to PrP^C. (A) Demonstration of affinity of Hsp60 for PrP^C by pull-down assay with Hsp60-coated beads. Control was assessed with beads only, the addition of anti-Hsp60 antibody, or purified Hsp60. Precipitates were analyzed by immunoblotting with anti-PrP^C antibody. (B) Cell lysate or immunoprecipitates with anti-PrP^C antibody and affinity of PrP^C for Hsp60 by pull-down assay with PrP^C-coated beads was analyzed by immunoblotting with anti-Hsp60 antibody. Control was assessed with beads only, or the addition of purified PrP^C. (C) Silver staining of precipitates by pull-down assay. Samples were purified with Hsp60 (control) and precipitates of pull-down with Hsp60-coated beads (PD). (D) Labeling of internalized bacteria in macrophages with antibody specific for Hsp60. Macrophages were incubated with *B. abortus* for 5 or 15 min, and Hsp60 were localized by immunofluorescence as described in Materials and Methods. Fluorescence microscopy of stained GFP-expressed wild-type strain with anti-Hsp60 and phase contrast microscopy of the corresponding microscopic fields are shown. Arrows point to bacteria.

not replicate in the macrophages from Ngsk PrP^C-deficient mice (Fig. 7 G). Macrophages from parent and Ngsk PrP^C-deficient mice showed no significant difference in the internalization, macropinosome formation, and intracellular replication of *virB4* mutant (Fig. 7, A–F and H). In macrophages from Ngsk PrP^C-deficient mice, wild-type strain failed to block phagosome maturation as shown by colocalization of phagosomes containing the bacteria and the late endocytic marker, LAMP-1, at 35 min after infection (Fig. 8, A and C). In contrast, wild-type strain prevented phagosome-lysosome fusion, and therefore phagosomes containing wild-type strain do not have LAMP-1 in macrophages from parent mice (Fig. 8, A and B).

To determine if this defect in intracellular replication of *B. abortus* correlates with an inability to establish infection in the host, we experimentally infected parent or PrP^C-deficient mice with *B abortus*. Many bacteria were recovered from the spleen of BALB/c and C57BL/6 mice infected with wild-type strain at 10 d after infection, but few bacteria were recovered from PrP^C-deficient mice, based on the number of CFUs in each spleen (Fig. 7 I). As previously reported (14), fewer bacteria were recovered from the spleen of three mice strains infected with *virB4* mutant (Fig. 7 I). These results suggested that replicative phagosome formation and proliferation in mice of *B. abortus* required the uptake pathway associated with PrP^C.

Several of the phenotypes ascribed to Ngsk PrP^C-deficient mice are most likely caused by up-regulation of prion protein (PrP)-like protein doppel rather than by ablation of PrP^C (27). To investigate the involvement of doppel expression on *B. abortus* infection, Zrch PrP^C-deficient mice (17), with no up-regulation of doppel, were used for infection assay. The results showed that phenotypes of Zrch PrP^C-deficient mice were almost the same as Ngsk PrP^C-deficient mice on *B. abortus* infection (Fig. 7 G). In addition, PrP^C transgenic Ngsk PrP^C-deficient mice were successfully rescued from the inhibition of bacterial intracellular growth (Fig. 7 G). Therefore, doppel expression was not involved in *B. abortus* infection.

Discussion

In this study, we have shown that Hsp60 of *B. abortus*, secreted on the bacterial surface by the type IV secretion

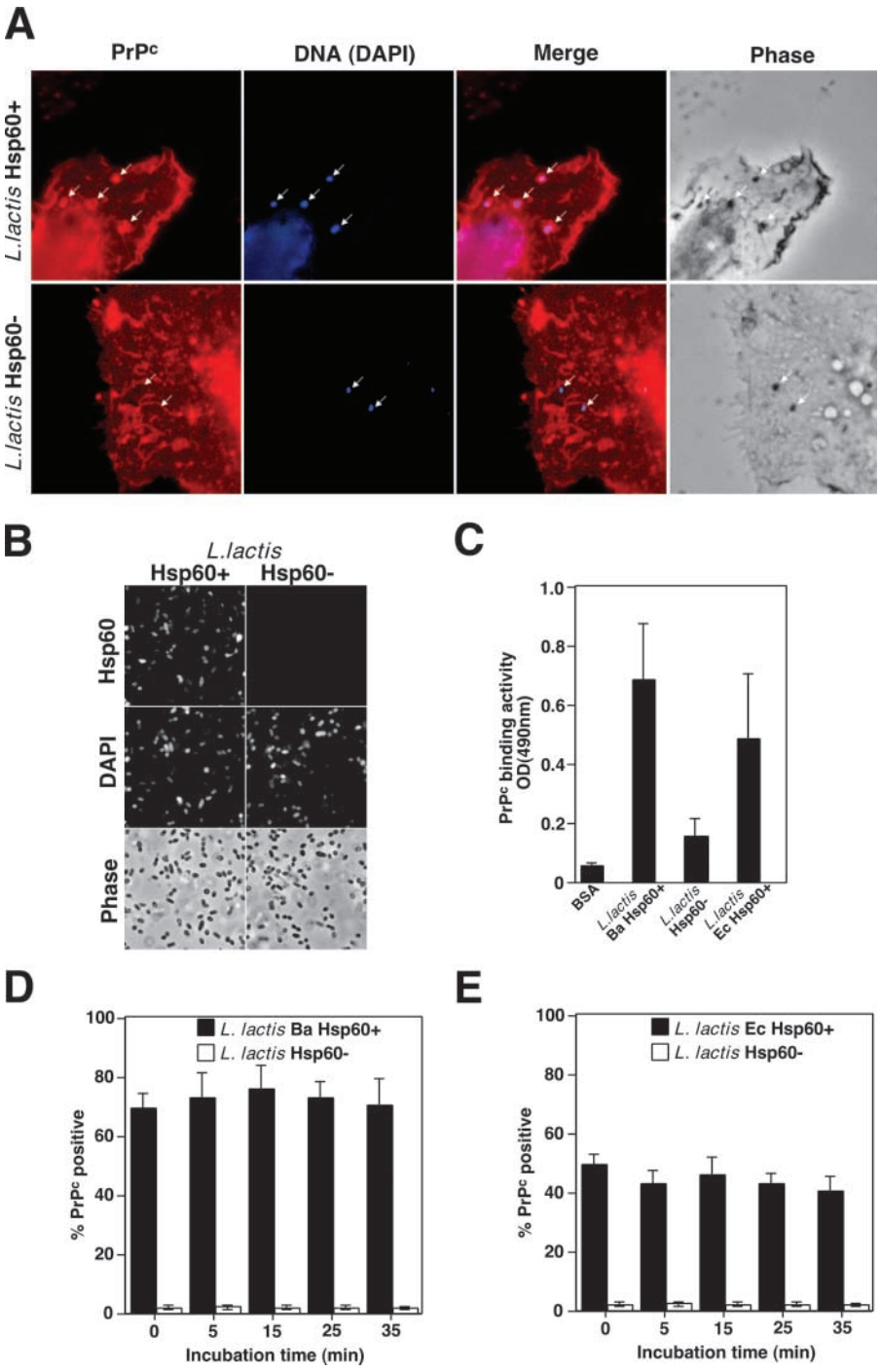

Figure 5. Aggregation of PrP^C by Hsp60 expressed on the surface of *L. lactis*. Macrophages were incubated with surface $Hsp60^+$ (top) or $Hsp60^-$ (bottom) *L. lactis* for 5 min, and PrP^C was localized by immunofluorescence as described in Materials and Methods. Phase contrast microscopy of the corresponding microscopic fields are shown. Bacteria (shown by arrows) were stained with DAPI. (B) Labeling of *L. lactis* grown in vitro, with antibody specific for Hsp60. Fluorescence microscopy of stained surface $Hsp60^+$ or $Hsp60^-$ *L. lactis* with anti-Hsp60 (top) or DAPI (middle) and phase contrast microscopy of the corresponding microscopic fields (bottom) are shown. (C) PrP^C-binding activity. Measurement of PrP^C-binding activity was performed by ELISA (refer to Materials and Methods). (D and E) Macrophages were incubated with surface $Hsp60^+$ (solid bars) or $Hsp60^-$ (open bars) *L. lactis* for the indicated time, and association of PrP^C was determined by immunofluorescence microscopy. Hsp60 of *B. abortus* (D) or *E. coli* (E) is expressing on *L. lactis* surface. % PrP^C positive refers to percentage of bacteria that showed costaining with PrP^C. 100 bacteria were examined per coverslip. Data are the average of triplicate samples from three identical experiments, and the error bars represent the standard deviation.

system–associated manner, interacted directly or indirectly with PrP^C, and that the interaction contributed to establish *B. abortus* infection. The cellular function of PrP^C is unclear. Our results in this study provide a novel aspect of PrP^C function as a receptor for an intracellular pathogen. Hsp60s, a member of the GroEL family of chaperonins in *E. coli*, is widely distributed and conserved between prokaryotes and mammals (28). Hsp60 proteins have been recognized as immunodominant antigens of many microbial pathogens, including *B. abortus* (22, 29). Hsp60s are believed to reside in the cytoplasm (30). However, surface-exposed Hsp60 has been reported in *Legionella pneumophila* and shown to be involved in pathogenicity (31). Presumably, Hsp60 of *L. pneumophila* binds to unknown receptors on nonprofessional phagocyte HeLa cells, initiating actin polymerization and endocytosis of the bacterium into an early endosome (32). But the role of surface-exposed Hsp60 in professional phagocytes, such as macrophages, is still unclear. As *L. pneumophila* has a type IV secretion system, surface expression of Hsp60 of *L. pneumophila* might

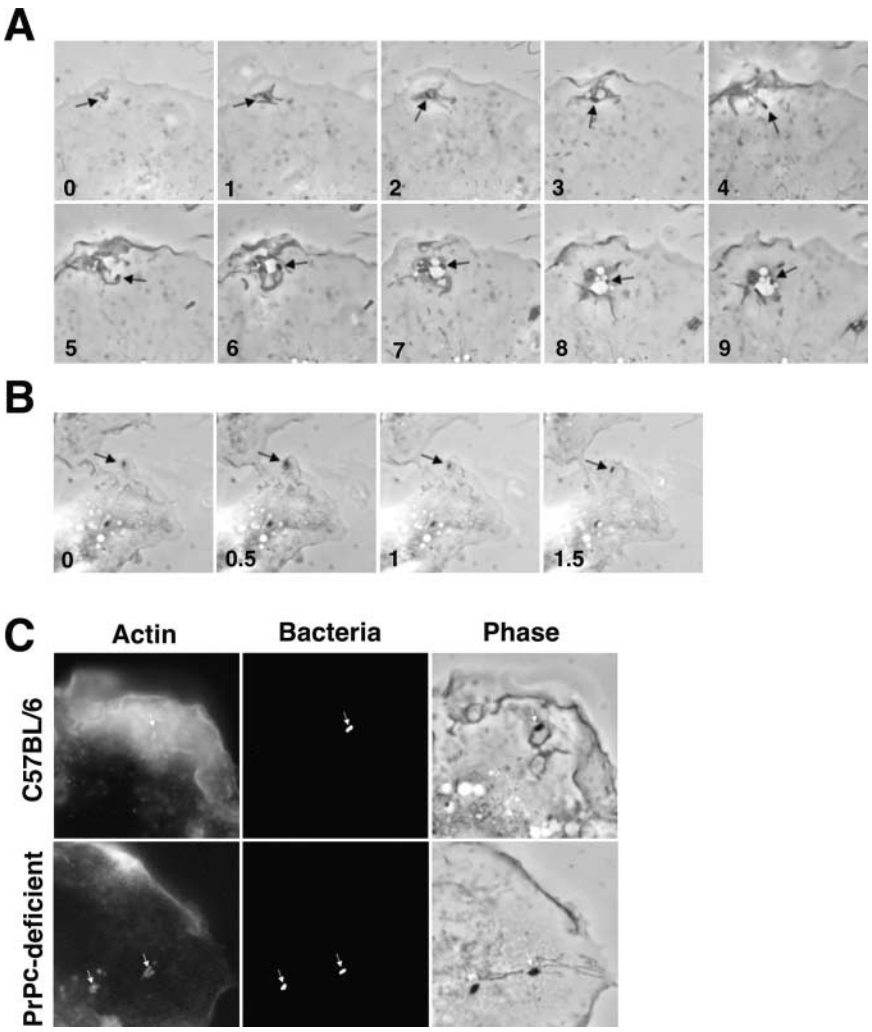

Figure 6. PrP^C-regulated swimming internalization of *B. abortus*. (A and B) Selected time lapse videomicroscopic images of wild-type *B. abortus* entry into macrophages from normal (A) or PrP^C-deficient C57BL/6 mice (B). Elapsed time in minutes is indicated at the bottom of each frame. Arrows point to bacteria. (C) Generalized actin polymerization after contact of macrophages with *B. abortus*. Bacteria were deposited onto macrophages from normal (top) or PrP^C-deficient mice (bottom) and then incubated for 5 min, fixed, and stained for actin filaments. Phase contrast microscopy of the corresponding microscopic fields are shown. Arrows point to bacteria.

be a similar mechanism to that of *B. abortus*. Effector proteins secreted by the type IV system of *B. abortus* have not been identified and this study is the first report describing a candidate effector-like protein secreted by the type IV system of *B. abortus*. Hsp60 are major antigens that elicit strong antibody responses in many bacteria (29). This includes bacteria that lack the type IV secretion system. Therefore, there is a possibility that Hsp60 might release by another secretion system and bind a denatured part of an effector protein of the type IV secretion system that might carry the Hsp60 to the bacterial surface.

It has been reported that PrP^C interacts with Hsp60 by using a *Saccharomyces cerevisiae* two-hybrid screening system (33). The PrP is the causative agent of neurodegenerative diseases such as Creutzfeld-Jakob disease in humans, bovine spongiform encephalopathy, and scrapie in sheep (34). The pathological, infectious form, PrP^{Sc}, is a β sheet aggregate, whereas the normal cellular isoform, PrP^C, consists of a largely α helical, autonomously folded COOH-terminal domain and an NH_2-terminal segment that is unstructured in solution (35). Conformational conversion of PrP^C into PrP^{Sc} has been suggested to involve a chaperone-like factor. GroEL of *E. coli* can catalyze the aggregation of chemically denatured and of folded, recombinant PrP in a model reaction in vitro (36). Based on a previous report, it was thought that surface-exposed Hsp60 of *B. abortus* could bind to PrP^C and catalyze the aggregation of PrP^C on macrophages. Consistent with this hypothesis, Hsp60 expressed on *L. lactis* could catalyze the aggregation of PrP^C on macrophages. However, PrP^C tail formation was not observed in macrophages infected with $Hsp60^+$ *L. lactis*. Hsp60 is not sufficient for PrP^C tail formation. In addition, swimming internalization and macropinosome formation were not observed in macrophages infected with $Hsp60^+$ *L. lactis*. PrP^C tail formation was required for bacterial swimming on macrophages and another bacterial factor, secreted by the type IV system, appears to be required for PrP^C tail formation.

B. abortus internalizes into macrophages by swimming on the cell surface for several minutes, with membrane sorting occurring during this period (6, 37). PrP^C tail formation is involved in the signaling pathway for swimming internalization because the PrP^C tail colocalized with Grb2 (unpublished data). Recently, evidence that PrP^C interacts

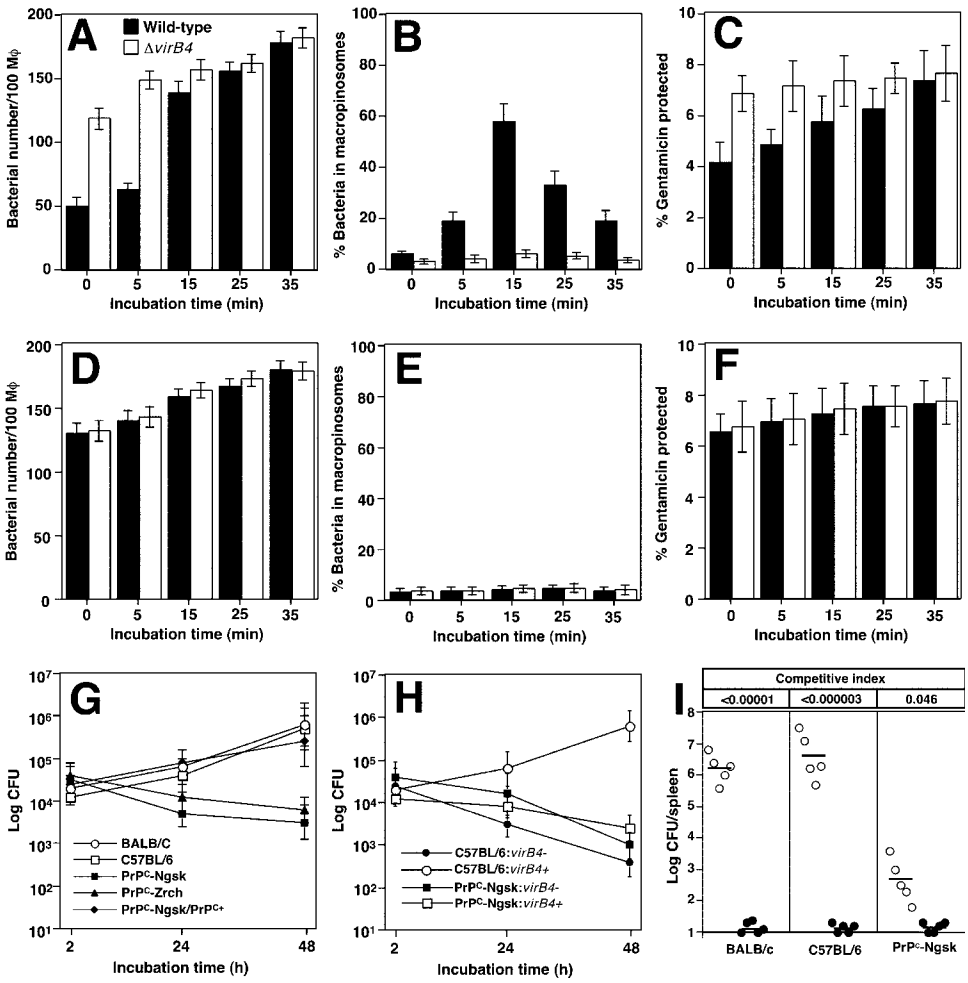

Figure 7. PrP^C-influenced *B. abortus* infection. (A–F) Wild-type (solid bars) or *virB4* mutant (open bars) were deposited onto macrophages from normal (A–C) or Ngsk PrP^C-deficient mice (D–F), and then incubated for the periods of time indicated. Uptake (A, C, D, and F) and macropinosome formation (B and E) were quantified as described in Materials and Methods. (A, B, D, and E) 100 macrophages were examined per coverslip. (C and F) Uptake efficiency by macrophages was determined by protection of internalized bacteria from gentamicin killing. Data are the average of triplicate samples from three identical experiments, and the error bars represent the standard deviation. (G and H) Intracellular replication of *B. abortus*. Macrophages from BALB/c, C57BL/6, Ngsk, or Zrch PrP^C-deficient mice, or PrP^C transgenic Ngsk PrP^C-deficient mice were infected with wild-type *B. abortus* (G), or *virB4* mutant (*virB4*−) and complemented strain (*virB4*+). (H). Data points and error bars represent the mean CFUs of triplicate samples from a typical experiment (performed at least four times) and their standard deviation, respectively. (I) Proliferation in mice. The CFUs of each strain were enumerated in the spleens of five mice from each group at 10 d after infection. For each mouse, the results are indicated by one open circle (log CFU of the wild-type) and one solid circle (log CFU of the *virB4* mutant). The means of the data are indicated by horizontal lines. The competitive index was calculated by dividing the mean ratio of mutant CFUs to the wild-type CFUs recovered from spleens by the ratio of the mutant CFUs to the wild-type CFUs in the inoculum.

with Grb2 was provided by the two-hybrid screening system (38). Grb2 is an adaptor protein involved in intracellular signaling from extracellular or transmembrane receptors to intracellular signaling molecules (39). The structure of Grb2 consists of a central SH2 domain flanked by two SH3 domains. The SH2 domain is responsible for interaction with tyrosine kinase, whereas the SH3 domains can bind to proline-rich motifs (40). Grb2 interacts through its SH3 domains with Wiskott-Aldrich syndrome protein (WASP), which plays a role in regulation of the actin cytoskeleton (41). WASP is a 64-kD protein expressed exclusively in hematopoietic cells (42). The carboxyl terminal portion of WASP contains regions that show homology to several actin-binding proteins, such as verprolin and cofilin, which may allow binding of WASP to filamentous actin (43). In regard to internalization of *B. abortus*, surface-exposed Hsp60 of *B. abortus* promotes aggregation of PrP^C, and PrP^C tail formation is induced by unidentified factor(s) secreted by the type IV system. The interaction of PrP^C tail with Grb2 will initiate cytoskeletal rearrangement and induce generalized membrane ruffling. Bacteria may obtain driving force for swimming internalization from membrane ruffling, like riding the wave of membrane until enclosed in macropinosomes. Consistent with this hypothesis, Grb2, which had interacted with PrP^C tail, was excluded in macropinosomes containing *B. abortus* (unpublished data). Presumably, the signal mediated by Grb2 is not required for replicative phagosome formation after macropinosome formation. Instead, a signal mediated by lipid rafts is needed for replicative phagosome formation (6).

The function of the *B. abortus virB* locus is essential for intracellular survival, both in cultured cells and in the mouse model (10, 11, 44–46). Our results of virulence for mice confirmed these previous works. The role of mouse macrophages in mediating resistance or susceptibility among mouse strains to some intracellular pathogens has been shown by studies of the *Ity/Lsh/Bcg* resistance model. Resistance to *Salmonella enterica* serovar Typhimurium, *Leishmania donovani*, and mycobacterial species is regulated by polymorphism of the *Nramp1* gene that controls macrophage function (47). Bovine Nramp1 is a major candidate for controlling the in vivo–resistant phenotype against *B. abortus* infection (48). Our previous study indicated that Niemann-Pick type C1 gene (NPC1) regulated the inter-

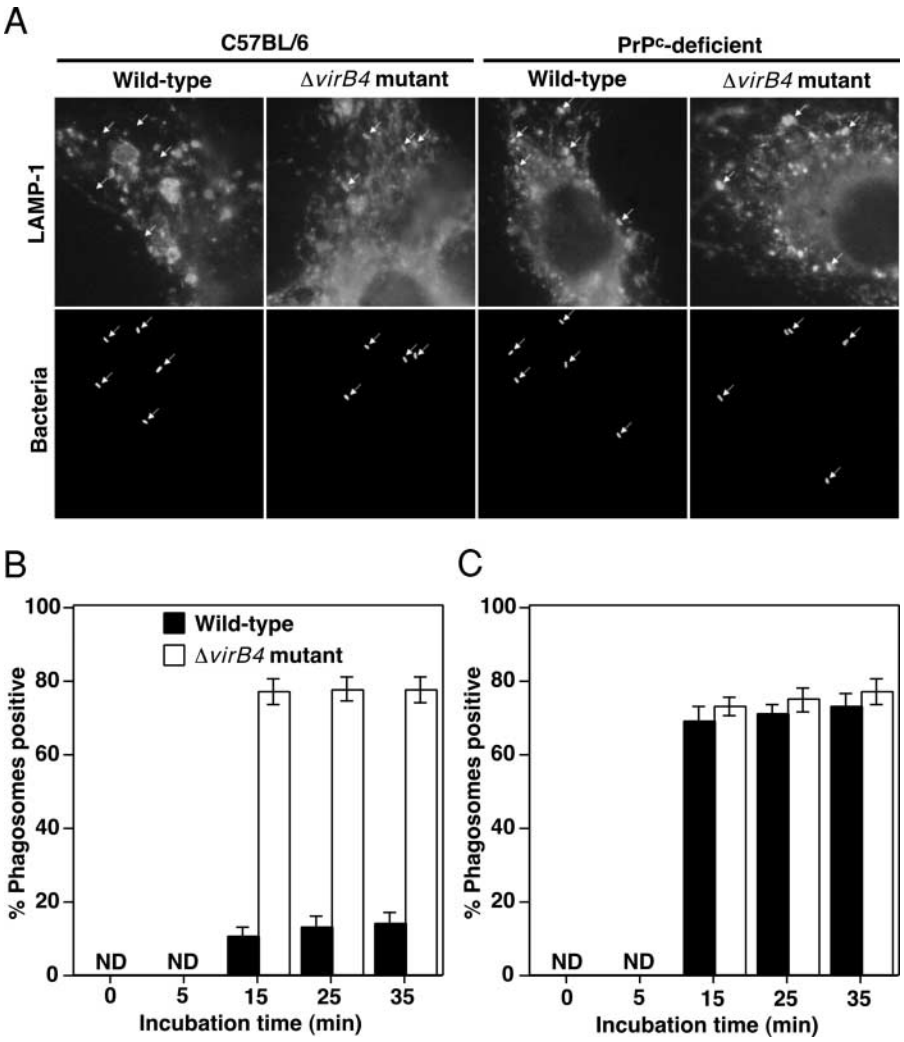

Figure 8. Colocalization of *B. abortus* with late endosomal and lysosomal marker LAMP-1 in macrophages from PrP^C-deficient mice, assessed by immunofluorescence microscopy. (A) Macrophages from C57BL/6 or PrP^C-deficient C57BL/6 mice were infected with wild-type or *virB4* mutant *B. abortus* for 35 min. (B and C) Wild-type (solid bars) or *virB4* mutant (open bars) were deposited onto macrophages from normal (B) or PrP^C-deficient mice (C), and then incubated for the periods of time indicated and probing with LAMP-1 was performed. % Phagosomes positive refers to percentage of internalized bacteria that showed costaining with LAMP-1, based on observation of 100 bacteria per coverslip. Data are the average of triplicate samples from three identical experiments, and error bars represent the standard deviation. ND, not detectable.

nalization and intracellular replication of *B. abortus* and also contributed to bacterial proliferation in mice (49). Macrophages from NPC1-deficient mice did not support internalization and intracellular replication of *B. abortus* (49). In this study, inhibition of internalization was not observed in macrophages from PrP^C-deficient mice. In NPC1-deficient mice macrophages, lipid raft-associated molecules, such as cholesterol, GM1 ganglioside, and GPI-anchored proteins, accumulated only in intracellular vesicles (49). In contrast, these molecules were present in both plasma membrane and intracellular vesicles of macrophages from PrP^C-deficient mice as well as macrophages from parent mice (unpublished data). Therefore, lipid raft-associated molecules on the plasma membrane are essential for the internalization of *B. abortus*, and PrP^C promotes the bacterial swimming internalization.

Lipid rafts are involved in infection by several intracellular pathogens. For example, macropinosomes containing *L. pneumophila* included lipid raft-associated molecules (50). GPI-anchored proteins were present in *Toxoplasma gondii* and *Plasmodium falciparum* vacuoles (51, 52). The intracellular parasite *L. donovani* can actively inhibit the acquisition of flotillin-1–enriched lipid rafts by phagosomes and the maturation of these organelles (53). Lipid platforms have been implicated in the budding of HIV and influenza virus (54, 55). The compartmentalization of Ebola and Marburg viral proteins within lipid rafts during viral assembly and budding has also been shown (56). In addition, PrP was attached to membranes by a GPI-anchor that associated with lipid rafts, and a recent study showed that conversion of raft-associated PrP^C to the protease-resistant state required insertion of PrP^{Sc} into contiguous membrane (57). Thus, lipid rafts, including PrP^C, may have an important role as a gateway for the intracellular trafficking of pathogens (58).

Current treatment of acute brucellosis requires combined regimen of antibiotics and is conditioned by the fact that brucellae are facultative intracellular pathogen. Thus, it is important to treat patients with drugs that penetrate macrophages. This fact seems to be responsible for the long duration of the disease and the high incidence of relapses. To this end, the study of the immunogenicities of antigens and their use in combination with new systems is very important for the development of better vaccines or antimicrobial agents. New strategies are also necessary to prevent brucel-

losis while avoiding the disadvantages of the currently used live vaccines for animals. The study of host–pathogen molecular interactions raises the possibility of novel vaccines or antimicrobial agents. The results of our study thus provide a potential new target for prevention of infection by intracellular pathogens.

We wish to thank Drs. Ben Adler and Hyeng-il Cheun for critical reading of the manuscript, Drs. Stanley B. Prusiner and Patrick Tremblay for PrP^C-deficient mice, and Drs. Chihiro Sasakawa and Toshihiko Suzuki for valuable discussion.

This work was supported, in part, by grants from The 21st Century Center of Excellence Program (A-1) and Scientific Research (12575029 and 13770129), Japan Society for the Promotion of Science.

Submitted: 15 November 2002
Revised: 23 April 2003
Accepted: 23 April 2003

References

1. Acha, P., and B. Szylres. 1980. Zoonosis and Communicable Diseases Common to Man and Animals. Pan American Health Organization, Washington, DC. pp. 28–45.
2. Zavala, I., A. Nava, J. Guerra, and C. Quiros. 1994. Brucellosis. *Infect. Dis. Clin. North Am.* 8:225–241.
3. Baldwin, C.L., and A.J. Winter. 1994. Macrophages and *Brucella*. *Immunol. Ser.* 60:363–380.
4. Comerci, D.J., M.J. Martinez-Lorenzo, R. Sieira, J. Gorvel, and R.A. Ugalde. 2001. Essential role of the VirB machinery in the maturation of the *Brucella abortus*-containing vacuole. *Cell. Microbiol.* 3:159–168.
5. Pizarro-Cerda, J., E. Moreno, V. Sanguedolce, J.L. Mege, and J.P. Gorvel. 1998. Virulent *Brucella abortus* prevents lysosome fusion and is distributed within autophagosome-like compartments. *Infect. Immun.* 66:2387–2392.
6. Watarai, M., S.-I. Makino, Y. Fujii, K. Okamoto, and T. Shirahata. 2002. Modulation of *Brucella*-induced macropinocytosis by lipid rafts mediates intracellular replication. *Cell. Microbiol.* 4:341–356.
7. Naroeni, A., and F. Porte. 2002. Role of cholesterol and the ganglioside GM(1) in entry and short-term survival of *Brucella suis* in murine macrophages. *Infect. Immun.* 70:1640–1644.
8. Christie, P.J., and J.P. Vogel. 2000. Bacterial type IV secretion: conjugation systems adapted to deliver effector molecules to host cells. *Trends Microbiol.* 8:354–360.
9. Delrue, R.M., M. Martinez-Lorenzo, P. Lestrate, I. Danese, V. Bielarz, P. Mertens, X. De Bolle, A. Tibor, J.P. Gorvel, and J.J. Letesson. 2001. Identification of *Brucella* spp. genes involved in intracellular trafficking. *Cell. Microbiol.* 3:487–497.
10. Sieira, R., D.J. Comerci, D.O. Sanchez, and R.A. Ugalde. 2000. A homologue of an operon required in *Brucella abortus* for virulence and intracellular multiplication. *J. Bacteriol.* 182: 4849–4855.
11. O'Callaghan, D., C. Cazevieille, A. Allardet-Servent, M.L. Boschiroli, G. Bourg, V. Foulongne, P. Frutos, Y. Kulakov, and M. Ramuz. 1999. A homologue of the *Agrobacterium tumefaciens* VirB and *Bordetella pertussis* Ptl type IV secretion systems is essential for intracellular survival of *Brucella suis*. *Mol. Microbiol.* 33:1210–1220.
12. Horiuchi, M., N. Yamazaki, T. Ikeda, N. Ishiguro, and M. Shinagawa. 1995. A cellular form of prion protein (PrPC) exists in many non-neuronal tissues of sheep. *J. Gen. Virol.* 76:2583–2587.
13. Erdenebaatar, J., S. Sugar, A. Yondondorj, T. Nagabayashi, B. Shuto, M. Watarai, S.-I. Makino, and T. Shirahata. 2002. Serological analysis of *Brucella*-vaccinated and -infected domesticated animals by using the agar gel immunodiffusion test with *Brucella* polysaccharide in Mongolia. *J. Vet. Med. Sci.* 64: 839–841.
14. Watarai, M., S.-I. Makino, and T. Shirahata. 2002. An essential virulence protein of *Brucella abortus*, VirB4, requires an intact nucleoside triphosphate-binding domain. *Microbiology.* 148:1439–1446.
15. Kovach, M.E., P.H. Elzer, D.S. Hill, G.T. Robertson, M.A. Farris, R.M. Roop, II, and K.M. Peterson. 1995. Four new derivatives of the broad-host-range cloning vector pBBR1MCS, carrying different antibiotic-resistance cassettes. *Gene.* 166:175–176.
16. Sakuguchi, S., S. Katamine, N. Nishida, R. Moriuchi, K. Shigematsu, T. Sugimoto, A. Nakatani, Y. Kataoka, T. Houtani, S. Shirabe, et al. 1996. Loss of cerebellar Purkinje cells in aged mice homozygous for a disrupted PrP gene. *Nature.* 380:528–531.
17. Bueler, H., M. Fischer, Y. Lang, H. Bluethman, H.P. Lipp, S.J. DeArmond, S.B. Prusiner, M. Aguet, and C. Weissmann. 1992. Normal development and behaviour of mice lacking the neuronal cell-surface PrP protein. *Nature.* 356: 577–582.
18. Nishida, N., P. Tremblay, T. Sugimoto, K. Shigematsu, S. Shirabe, C. Petromilli, S.P. Erpel, R. Nakaoke, R. Atarashi, T. Houtani, et al. 1999. A mouse prion protein transgene rescues mice deficient for the prion protein gene from Purkinje cell degeneration and demyelination. *Lab. Invest.* 79:689–697.
19. Watarai, M., S. Funato, and C. Sasakawa. 1995. Interaction of Ipa proteins of *Shigella flexneri* with $\alpha5\beta1$ integrin promotes entry of the bacteria into mammalian cells. *J. Exp. Med.* 183:991–999.
20. Horiuchi, M., G.S. Baron, L.W. Xiong, and B. Caughey. 2001. Inhibition of interactions and interconversions of prion protein isoforms by peptide fragments from the C-terminal folded domain. *J. Biol. Chem.* 276:15489–15497.
21. Satoh, E., Y. Ito, Y. Sasaki, and T. Sasaki. 1997. Application of the extracellular alpha-amylase gene from *Streptococcus bovis* 148 to construction of a secretion vector for yogurt starter strains. *Appl. Environ. Microbiol.* 63:4593–4596.
22. Roop, R.M., II, M.L. Price, B.E. Dunn, S.M. Boyle, N. Sriranganathan, and G.G. Schurig. 1992. Molecular cloning and nucleotide sequence analysis of the gene encoding the immunoreactive *Brucella abortus* Hsp60 protein, BA60K. *Microb. Pathog.* 12:47–62.
23. Hemmingsen, S.M., C. Woolford, S.M. van der Vies, K. Tilly, D.T. Dennis, C.P. Georgopoulos, R.W. Hendrix, and R.J. Ellis. 1988. Homologous plant and bacterial proteins chaperone oligomeric protein assembly. *Nature.* 333:330–334.
24. Holo, H., and I.F. Nes. 1989. High-frequency transformation by electroporation of *Lactococcus lactis* subsp. *cremoris* grown with glycine in osmotically stabilized media. *Appl. Environ. Microbiol.* 57:333–340.
25. Watarai, M., H.L. Andrews, and R.R. Isberg. 2001. Formation of a fibrous structure on the surface of *Legionella pneumophila* associated with exposure of DotH and DotO proteins after intracellular growth. *Mol. Microbiol.* 39:313–329.

26. Abrami, L., M. Fivaz, P.E. Glauser, R.G. Parton, and F.G. van der Goot. 1998. A pore-forming toxin interacts with a GPI-anchored protein and causes vacuolation of the endoplasmic reticulum. *J. Cell Biol.* 140:525–540.
27. Moore, R.C., I.Y. Lee, G.L. Silverman, P.M. Harrison, R. Strome, C. Heinrich, A. Karunaratne, S.H. Pasternak, M.A. Chishti, Y. Liang, et al. 1999. Ataxia in prion protein (PrP)-deficient mice is associated with upregulation of the novel PrP-like protein doppel. *J. Mol. Biol.* 292:797–817.
28. Bukau, B., and A.L. Horwich. 1998. The Hsp70 and Hsp60 chaperone machines. *Cell.* 92:351–366.
29. Kaufmann, S.H. 1990. Heat shock proteins and the immune response. *Immunol. Today.* 11:129–136.
30. Craig, E.A., B.D. Gambill, and R.J. Nelson. 1993. Heat-shock proteins: molecular chaperones of protein biogenesis. *Microbiol. Rev.* 57:402–414.
31. Hoffman, P.S., and R.A. Garduno. 1999. Surface-associated heat shock proteins of *Legionella pneumophila* and *Helicobactor pylori*: roles in pathogenesis and immunity. *Infect. Dis. Obstet. Gynecol.* 7:58–63.
32. Garduno, R.A., E. Garduno, and P.S. Hoffman. 1998. Surface-associated Hsp60 chaperonin of *Legionella pneumophila* mediates invasion in a HeLa cell model. *Infect. Immun.* 66: 4602–4610.
33. Edenhofer, F., R. Rieger, M. Famulok, W. Wendler, S. Weiss, and E.-L. Winnacker. 1996. Prion protein PrP^C interacts with molecular chaperones of the Hsp60 family. *J. Virol.* 70:4724–4728.
34. Prusiner, S.B. 1998. Prions. *Proc. Natl. Acad. Sci. USA.* 95: 13363–13383.
35. Jackson, G.S., and A.R. Clarke. 2000. Mammalian prion proteins. *Curr. Opin. Struct. Biol.* 10:69–74.
36. Stockel, J., and F.U. Hartl. 2001. Chaperonin-mediated *de novo* generation of prion protein aggregates. *J. Mol. Biol.* 313: 861–872.
37. Kim, S., M. Watarai, S.-I. Makino, and T. Shirahata. 2002. Membrane sorting during swimming internalization of *Brucella* is required for phagosome trafficking decisions. *Microb. Pathog.* 33:225–237.
38. Spielhaupter, C., and H.M. Schatzl. 2001. PrP^C directly interacts with proteins involved in signaling pathways. *J. Biol. Chem.* 276:44604–44612.
39. Koch, C.A., D. Anderson, M.F. Moran, C. Ellis, and T. Pawson. 1991. SH2 and SH3 domains: elements that control interactions of cytoplasmic signaling proteins. *Science.* 252: 668–674.
40. Anderson, D., C.A. Koch, L. Grey, C. Ellis, M.F. Moran, and T. Pawson. 1990. Binding of SH2 domains of phospholipase C gamma 1, GAP, and Src to activated growth factor receptors. *Science.* 250:979–982.
41. She, H.Y., S. Rockow, J. Tang, R. Nishimura, E.Y. Skolnik, M. Chen, B. Margolis, and W. Li. 1997. Wiskott-Aldrich syndrome protein is associated with the adapter protein Grb2 and the epidermal growth factor receptor in living cells. *Mol. Biol. Cell.* 8:1709–1721.
42. Stewart, D.M., S. Treiber-Held, C.C. Kurman, F. Facchetti, L.D. Notarangelo, and D.L. Nelson. 1996. Studies of the expression of the Wiskott-Aldrich syndrome protein. *J. Clin. Invest.* 97:2627–2634.
43. Derry, J.M., H.D. Ochs, and U. Francke. 1994. Isolation of a novel gene mutated in Wiskott-Aldrich syndrome. *Cell.* 78: 635–644.
44. Foulongne, V., G. Boug, C. Cazavieille, S. Michaux-Charachon, and D. O'Callaghan. 2000. Identification of *Brucella suis* genes affecting intracellular survival in an in vitro human macrophage infection model by signature-tagged transposon mutagenesis. *Infect. Immun.* 68:1297–1303.
45. Hang, P.C., R.M. Tsolis, and T.A. Ficht. 2000. Identification of genes required for chronic persistence of *Brucella abortus* in mice. *Infect. Immun.* 68:4102–4107.
46. Sum, Y.-H., A.B. den Hartigh, R. de Lima Santos, L.G. Adams, and R.M. Tsolis. 2002. *virB*-mediated survival of *Brucella abortus* in mice and macrophages is independent of a functional inducible nitric oxide synthase or NADPH oxidase in macrophages. *Infect. Immun.* 70:4826–4832.
47. Forbes, J.R., and P. Gros. 2001. Divalent-metal transport by NRAMP proteins at the interface of host-pathogen interactions. *Trends Microbiol.* 9:397–403.
48. Barthel, R., J. Feng, J.A. Piedrahita, D.N. McMurray, J.W. Templeton, and L.G. Adams. 2001. Stable transfection of the bovine *NRAMP1* gene into murine RAW264.7 cells: effect on *Brucella abortus* survival. *Infect. Immun.* 69:3110–3119.
49. Watarai, M., S.-I. Makino, M. Michikawa, K. Yanagisawa, S. Murakami, and T. Shirahata. 2002. Macrophage plasma membrane cholesterol contributes to *Brucella abortus* infection of mice. *Infect. Immun.* 70:4818–4825.
50. Watarai, M., I. Derre, J. Kirby, J.D. Growney, W.F. Dietrich, and R.R. Isberg. 2001. *Legionella pneumophila* is internalized by a macropinocytotic uptake pathway controlled by the Dot/Icm system and the mouse *Lgn1* locus. *J. Exp. Med.* 194:1081–1095.
51. Mordue, D.G., N. Desai, M. Dustin, and L.D. Sibley. 1999. Invasion by *Toxoplasma gondii* establishes a moving junction that selectively excludes host cell plasma membrane proteins on the basis of their membrane anchoring. *J. Exp. Med.* 190: 1783–1792.
52. Lauer, S., J. VanWye, T. Harrison, H. McManus, B.U. Samuel, N.L. Hiller, N. Mohandas, and K. Haldar. 2000. Vacuolar uptake of host components, and a role for cholesterol and sphingomyelin in malarial infection. *EMBO J.* 19:3556–3564.
53. Dermine, J.-F., S. Duclos, J. Garin, F. St-Louis, S. Rea, R.G. Parton, and M. Desjardins. 2001. Flotillin-1-enriched lipid raft domains accumulate on maturing phagosomes. *J. Biol. Chem.* 276:18507–18512.
54. Scheiffele, P., A. Rietveld, T. Wilk, and K. Simons. 1999. Influenza viruses select ordered lipid domains during budding from the plasma membrane. *J. Biol. Chem.* 274:2038–2044.
55. Nguyen, D.H., and J.E. Hildreth. 2000. Evidence for budding of human immunodeficiency virus type 1 selectively from glycolipid-enriched membrane lipid rafts. *J. Virol.* 74: 3264–3272.
56. Bavari, S., C.M. Bosio, E. Wiegand, G. Ruthel, A.B. Will, T.W. Geisbert, M. Hevey, C. Schmaljohn, A. Schmaljohn, and M.J. Aman. 2002. Lipid raft microdomains: a gateway for compartmentalized trafficking of Ebola and Marburg viruses. *J. Exp. Med.* 195:593–602.
57. Baron, G.S., K. Wehrly, D.W. Dorward, B. Chesebro, and B. Caughey. 2002. Conversion of raft associated prion protein to the protease-resistant state requires insertion of PrP-res (PrP(Sc)) into contiguous membranes. *EMBO J.* 21:1031–1040.
58. Duncan, M.J., J.-S. Shin, and S.N. Abraham. 2002. Microbial entry through caveolae: variations on a theme. *Cell. Microbiol.* 4:783–791.